12-2-2017

Endothelial Nitric Oxide Synthase Oxygenase on Lipid Nanodiscs: A Nano-Assembly Reflecting Native-Like Function of eNOS

Ghaith AlTawallbeh
Cleveland State University

Mohammad M. Haque
Cleveland Clinic Foundation

Kiril A. Streletzky
Cleveland State University, K.STRELETZKY@csuohio.edu

Dennis J. Stuehr
Cleveland Clinic Foundation

Mekki Bayachou
Cleveland State University, M.BAYACHOU@csuohio.edu

Endothelial Nitric Oxide Synthase Oxygenase on Lipid Nanodiscs: A Nano-assembly Reflecting Native-Like Function of eNOS

Ghaith Altawallbeh[1], **Mohammad M. Haque**[2], **Kiril A. Streletzky**[3], **Dennis J. Stuehr**[2], and **Mekki Bayachou**[1,2,*]

[1]Department of Chemistry, Cleveland State University, Cleveland, OH, USA

[2]Department of Pathobiology, Lerner Research Institute, The Cleveland Clinic, Cleveland, OH, USA

[3]Department of Physics, Cleveland State University, Cleveland, OH, USA

Abstract

Endothelial nitric oxide synthase (eNOS) is a membrane-anchored enzyme. To highlight the potential role and effect of membrane phospholipids on the structure and activity of eNOS, we have incorporated the recombinant oxygenase subunit of eNOS into lipid nanodiscs. Two different size distribution modes were detected by multi-angle dynamic light scattering both for empty nanodiscs, and nanodiscs-bound eNOS$_{oxy}$. The calculated hydrodynamic diameter for mode 1 species was 9.0 nm for empty nanodiscs and 9.8 nm for nanodisc bound eNOS$_{oxy}$. Spectroscopic Griess assay was used to measure the enzymatic activity. Remarkably, the specific activity of nanodisc-bound eNOS$_{oxy}$ is ~65% lower than the activity of free enzyme. The data shows that the nano-membrane environment affects the catalytic properties of eNOS heme domain.

Keywords

Nitric Oxide; eNOS oxygenase domain; nanodisc; membrane; enzyme activity

---

*To whom correspondence should be addressed. Prof. Dr. Mekki Bayachou, Department of Chemistry, Cleveland State University, 2399 Euclid Avenue, Cleveland, OH 44115, United States. Tel.: +1 216 875 9716; fax: +1 216 687 9298.

1. Introduction

Endothelial nitric oxide synthase (eNOS) is one member of NO producing family, and is the only membrane-associated isoform [1-3]. Some of the work published on the mechanisms of eNOS function was performed on culture cells. This was done in an effort to understand the various regulatory mechanisms and functions of eNOS at the cellular level, but the complexity of eNOS regulation along with several uncontrolled factors associated with culture cells is responsible for conflicting results. As a result, much of the regulatory mechanisms of this enzyme still remain elusive [4]. Another line of work used genetically engineered soluble forms in detergents, phospholipid vesicles, and liposomes without addressing the effect of phospholipid membranes on the enzyme's functionality. Previous studies showed that purified eNOS are able to bind some phospholipid types but were in disagreement regarding its activity [5-7].

Nanodiscs are discoidal phospholipid protein complexes that have been developed by Sligar's laboratory as model membranes [8]. These soluble nanoscale phospholipid bilayers can attach membrane-bound and membrane-associated molecules to study the protein's native function [9-11]. A number of membrane proteins have been successfully incorporated into nanodisc including P450 enzymes, which have striking similarities with the oxygenase domain of NOS enzymes [10]. For example, they both exhibit a heme-thiolate catalytic center that drives the overall oxidation reaction. In addition, others have shown that membrane proteins reconstituted into nanodiscs not only retain their activities but also have better activity in nanodiscs when compared to other membrane models [12-16]. For instance, the ATP-binding cassette transporter P-glycoprotein 1 displayed greater activity in nanodiscs than in liposomes [9]. Also the catalytic efficiencies of amine oxidation by recombinant human monoamine oxidase A appeared to be greater in comparison to detergent-based systems [16].

We report herein preliminary data on eNOS heme domain catalytic activity after incorporation into phospholipid nanodiscs for the first time. These nanodiscs provide a unique system that may mimic the enzyme's native microenvironment, yet the prepared enzyme/nanodiscs assemblies can be conveniently studied in solution like any soluble enzyme preparation. We also characterized the size distribution and shape of $eNOS_{oxy}$ in POPC-nanodiscs. Overall, our data served as a reference point to establish a well-defined system for full length eNOS incorporation. This work opens the avenue for testing different lipid composition, as well as possible role of cholesterol on eNOS activity.

2. Material and Methods

Palmitoyl-2-oleoyl-sn-glyero-3-phosphocholine (POPC) was purchased from Avanti Polar Lipids (Alabaster, AL). 10 kDa Amicon Ultra-filter (Millipore, Billerica MA). All other buffers and reagents were purchased in the highest grade available from Sigma unless specified otherwise. The plasmid encoding for recombinant endothelial nitric oxide synthase oxygenase domain was a generous gift of Dr. Stuehr's laboratory in the Lerner Institute of the Cleveland Clinic.

2.1 Expression and purification of MSP1E3D1

The plasmid pMSP1E3D1 was purchased from Addgene and transformed into *E. coli* strain BL21-Gold (DE3) competent cells (Stratagene). MSP1E3D1 was expressed in a bench top fermenter and purified by Ni^{2+}-nitrilotriacetate (NTA) affinity chromatography as previously described [9].

2.2 Expression and Purification of eNOS oxygenase domain

Wildtype eNOS oxygenase domain with a six-histidine tag were overexpressed in *E. coli* BL21(DE3) strain using pCWori vector and purified as reported previously by Ni^{2+}-NTA affinity column chromatography [17]. The ferrous heme–CO adduct absorbing at 444 nm was used to measure heme protein content with an extinction coefficient of $\varepsilon_{444} = 74$ mM^{-1} cm^{-1} (A_{444}–A_{500}) [18].

2.3 Preparation of empty and eNOS$_{oxy}$ incorporated nanodisc samples

Nanodisc and eNOS$_{oxy}$/nanodisc assembly procedures were performed following protocols developed by Sligar et al. Briefly, POPC lipids from a chloroform stock were dried under a stream of nitrogen gas and placed overnight in a vacuum-desiccator or for couple hours in a CentriVap concentrator to remove residual chloroform. The thin lipid films were resuspended using sodium cholate containing buffer to a final concentration of 50 mM. The mixture was then sonicated in cold water bath, placed on ice, and vortexed from time to time to ensure complete solubilization of the lipids. For empty nanodiscs, MSP1E3D1 was added to the mixture in a 1:130:260 molar ratios with POPC/cholate. For eNOS$_{oxy}$ loaded nanodiscs, the enzyme was added into a similar mixture mentioned above to give molar ratios of 0.1:1:130:260 eNOS$_{oxy}$: MSP1E3D1: POPC: cholate. The mixture was then incubated for approximately 1 h at 4 °C. Lastly, the self-assembly was initiated by dialyzing overnight against buffer 1 [20 mM Tris-HCl, 100 mM NaCl, 50 mM EDTA (pH 7.4)] to remove the detergent.

2.4 Dynamic Light Scattering (DLS) studies

Dynamic light scattering experiments were done using an Ar+ Spectra Physics 2017 laser with a wavelength of 514.5 nm and maximum power of 2 W. The sample cell was held in a decalinfilled quartz vat, and the temperature of the cell was set to 20 °C using a Neslab RTE-111 refrigerated water bath (± 0.2 °C). DLS experiments were carried out at scattering angles from 40° to 110° in increments of 5°. The incident laser light was vertically polarized by passing through Glan-Laser calcite polarizer (Thorlabs, GL 10). Vertically and horizontally polarized scattered light (VV and VH, correspondingly) was detected by a BI-DS2 photomultiplier with attached Precision Linear Polarizer (Newport 20LP-VIS-B). Measured photon counts were analyzed with BI-9000 digital correlator. The samples were drained out of the dialyzing cassettes and diluted with buffer 1 to a final volume of 1.2 ml. Then samples are passed through 0.22 μm filter membranes into dust-free pre-cleaned tubes. Measured correlation functions were fit to a sum of one or two stretched exponentials and their decay rates were analyzed with the help of spectral time moment analysis to obtain the average decay rate (Γ) of every distinct mode in a correlation functions and different scattering angles θ and, therefore, at different wave vectors q = $(4\pi n/\lambda \sin(\theta/2)$ where λ is

the wavelength of the laser and n is the refractive index of the dispersant. The average diffusion coefficients (D), was deduced from $\Gamma(q^2)$ dependences for diffusive modes (the ones for which $\Gamma(q^2)$ is linear with a small intercept). The apparent hydrodynamic radius was calculated for the diffusive modes.

2.5 Enzyme activity assays

UV-vis absorbance spectra were recorded on Agilent 8453 spectrometer for $eNOS_{oxy}$ concentration determination. The activity of $eNOS_{oxy}$ was determined using a Spectra max plus 384 plate reader based on the Griess reaction through a standard calibration curve. It quantifies NO in the form of nitrite (NO_2^-) in a two-step diazotization reaction in which acidified nitrite produces a nitrosating agent, which is then derivatized to produce the final azo-product with a maximum absorption at 540 nm.

Catalysis of nitric oxide production (in the form of nitrite) from N-hydroxyarginine (NOHA) and H_2O_2 by $eNOS_{oxy}$ and $eNOS_{oxy}$ bound nanodisc were assayed in 96-well microplates at 37 °C as described previously with modifications. Assays (50 μl final volume) contained 20 mM Tris, 100 mM NaCl, pH 7.4, 500 nM $eNOS_{oxy}$, 1 mM NOHA, 0.5 mM DTT, 30 mM H_2O_2, and 10 μM H_4B. Reactions were started by adding H_2O_2 and stopped after 10 min by adding catalase (1300 units). Griess reagents 50 μl of sulfanilamide was added and incubated for 10 min in dark followed by 50 μl of NED which was treated the same. Finally, the assay plate was read at 540 nm in a Spectra max plate reader. Nitrite production was quantitated based on $NaNO_2$ standards.

3. Results and Discussion

3.1 Assembly and purification of empty and eNOS$_{oxy}$ incorporated nanodisc samples

The oxygenase domain of eNOS was reconstituted into phospholipid nanodiscs for the first time under optimized experimental conditions. The purified $eNOS_{oxy}$, synthetic lipid, and recombinant membrane scaffold protein (MSP, specifically MSP1E3D1) variant [19] was used in stoichiometric ratios to prepare the nanoparticles. The self-assembly of $eNOS_{oxy}$ in a phospholipid bilayer is stabilized by the encircling amphipathic helical protein belt, which acts as a membrane scaffold protein (Figure 1).

Schematic representations for both $eNOS_{oxy}$ dimer and empty nanodisc were adapted from Protein Data Bank [20, 21]. The purification of recombinant MSP as well as $eNOS_{oxy}$ expression in *E. coli* was performed following standard protein purification protocols reported in the literature (Figures S1-S2).

The reconstitution of $eNOS_{oxy}$ into the lipid nanodiscs is performed *in situ* following a standard self-assembly protocol of POPC/cholate nanodiscs in the presence of $eNOS_{oxy}$ followed by dialysis [9]. To gain more insight on the behavior of $eNOS_{oxy}$ in these nanoparticles, we have studied its physical characteristics in heterogeneous samples. The size distributions of assembled particles are examined by its dynamic light scattering properties. Accordingly, this method will provide a new approach to study eNOS in solution but in a system that reflects its native association with a membrane. This will allow us to

better understand the structure-function relationship of eNOS in a native-like microenvironment.

3.2 Light scattering characterization

Light scattering characterization of the nanodiscs and eNOS$_{oxy}$/nanodiscs yielded reproducible correlation functions of the Vertical/Vertical (VV) signal that covered almost three decades of a decay indicating strong scattering by nanodiscs (Figure 2).

The light scattering results were found to be highly reproducible within first 2 days after fresh preparation of the samples. The same samples show changes in behavior after 4 days indicating signs of aggregation as expected from sample aging (Figure S3). The correlation functions obtained for both samples were not unimodal, indicating the presence of more than one population with size distributions reflecting the scattering species in each sample. None of the samples produced a measurable Vertical/Horizontal (VH) signal. For every sample the correlation functions were found to depend strongly on the scattering angle, consistent with translational motion of diffusive species.

The correlation functions for all samples were successfully fit by a sum of two stretched exponentials using non-linear least squares fit. Figure 3 shows an example of a fit for data obtained at 40° angle. Spectral time moment analysis of the correlation functions yielded the corresponding decay rates Γ for each of the observed modes.

Both nanodisc and eNOS$_{oxy}$/nanodiscs samples yield two modes, the faster of which (shown on Figure 3) had 70-80% contribution to the correlation function.

Both Γ reveal clearly diffusive $\Gamma(q^2)$ behavior (small intercepts < 0.5 %, almost pure exponential decays) [22]. Corresponding apparent hydrodynamic radii, R_h, were found to be 4.5 nm and 4.9 nm for nanodisc and eNOS$_{oxy}$/nanodisc samples, respectively. The faster modes in the two samples most likely represent empty and eNOS$_{oxy}$/nanodiscs. The slower modes of both nanodisc and eNOS$_{oxy}$-nanodisc contribute about 20-30% to the correlation function and show less diffusive character (significant intercepts ~10% and significant stretching of the exponential decay) [22, 23]. The apparent R_h corresponding to the slower modes in both cases is in the range of 33-35 nm. This mode likely corresponds to either coalesced nanodiscs or particle-like byproducts of nanodisc preparation.

Nanodisc diameter is controlled by the MSP variant used in the assembly. Data published on the optimal stoichiometry of POPC lipids per nanodisc using MSP1E3D1 protein variant showed nanodiscs of ~ 12.1 nm in diameter [9, 24]. It is important to mention that the average size of empty nanodiscs in the latter was determined by size exclusion chromatography (SEC) technique relying on molecular weight standards with coupled stokes diameters. In this study, we measured our hydrodynamic radius based on the diffusion coefficient of the molecules in solution using data of multi-angle dynamic light scattering (DLS). DLS measures the intensity of fluctuations of scattered light arising from moving particles and calculates the hydrodynamic radius from the diffusion coefficient using the Stokes Einstein equation [25-27]. Following this procedure, we were able to conclude that empty nanodiscs are 9.0 nm in diameter (R_h 4.5 nm) and eNOS$_{oxy}$/nanodiscs are ~10.0 nm

in diameter (R_h 4.9 nm). To further check if the discrepancy in diameters is simply due the methods used, we run a sample through SEC column calibrated with size standards (Supporting info, Figures S4-S6). The eluted MSP1E3D1 nanodiscs with and without eNOS$_{oxy}$ were estimated to have a hydrodynamic diameter of approximately 13.7 nm and 11.6 nm respectively (Supporting info, Table S1). This is not different from diameters reported by Bayburt and others who showed that hydrodynamic diameter of MSP1E3D1/ POPC nanodiscs by SEC with and without their target protein at 12.0 nm and 14.0 nm [19, 28, 29]. The advantage of the DLS approach is its ability to extract true hydrodynamic radii of freely diffusing species. Also, since the intensity of the scattered light is proportional to the sixth power of the radius [26], multi-angle DLS is able to detect small quantities of eNOS$_{oxy}$/nanodisc with good sensitivity. This route has not only saved time but also avoided losing enzyme activity from further purification steps.

Following the DLS analysis of eNOS$_{oxy}$/nanodiscs, we examined if the activity of eNOS$_{oxy}$ is affected when incorporated on lipid nanodiscs. To determine the specific activity of eNOS$_{oxy}$ enzymes in the free form and on nanodiscs we need to accurately measure the concentration of eNOS$_{oxy}$ in both cases.

3.3 Enzyme activity assays

We used the P450-shift assay [30] to determine the concentration of enzyme in each case. Briefly, the reduction of the enzyme in the ferric heme state and reaction with carbon monoxide (CO) results in the stoichiometric formation of ferrous carbonyl complex of the enzyme (Fe^{II}-CO heme complex) with a distinctive absorption at 444 nm (Supporting info, Figures S7). This adduct is used to measure hemoprotein content with and without nanodiscs using an extinction coefficient of $\varepsilon_{444} = 76$ mM^{-1} cm^{-1} [30].

We measured the enzyme's specific activity for free eNOS$_{oxy}$ and for eNOS$_{oxy}$/nanodisc assembly. To measure eNOS$_{oxy}$ enzymatic activity, we used the catalytic conversion of N-hydroxyarginine (NOHA) in the presence of hydrogen peroxide and other ingredients of NOS$_{oxy}$ activity [31]. The specific activity of eNOS$_{oxy}$/nanodisc or free eNOS$_{oxy}$ is calculated in nmol(NO)/min/nmol(enzyme) at 37°C. We measured the activity by quantifying nitric oxide produced in the form of nitrite based on the Griess assay reaction [17]. Figure 4 shows observed specific activities for free eNOS$_{oxy}$ versus eNOS$_{oxy}$ on nanodiscs under similar conditions. Our results show that the observed specific activity of nanodisc-bound eNOS$_{oxy}$ (49.0 ± 1.3) nmol/min/nmol is about 65% lower than that of the free eNOS$_{oxy}$ enzyme (132.4 ± 2.4) nmol/min/nmol. Our data suggest that the nanodisc microenvironment represses the catalytic properties of eNOS oxygenase.

In cells, eNOS is a membrane bound enzyme. In endothelial cells, eNOS seems to localize at cholesterol-rich microdomains such as caveolae [1, 32]. Studies showed that the eNOS microenvironment, the local lipid/cholesterol composition, and local membrane dynamics affect its overall catalytic function [33, 34]. In this work, while eNOS$_{oxy}$ on nanodiscs retained its ability to convert NOHA to NO under typical conditions of catalytic activity, it did so at a much lower activity (~65% lower than free eNOS$_{oxy}$). Before the advent of lipid nanodiscs, Venema and collaborators reported that wild type eNOS binds to phospholipid vesicles, and that the catalytic activity of the enzyme is affected by phospholipids as well as

by biological membranes isolated from cultured cells [35]. Differential eNOS activity has also been reported for eNOS localized in plasma membrane versus eNOS targeted to Golgi complex. Several cellular mechanisms may be at play for the functional difference between plasma membrane eNOS versus Golgi eNOS [36]. However, at the basic molecular level, the difference in phospholipid content between caveolae and Golgi membrane may in part explain the differential activity [37]. In fact, phospholipids in Golgi complex have been suspected in preventing eNOS activation [38]. Also, acute modulation of cholesterol levels in plasma membrane has been shown to dramatically affect the activity of eNOS [39]. This shows that the interactions of eNOS with molecular components of the local microenvironment affect its intrinsic catalytic activity. The decreased activity of eNOS oxygenase as a result of incorporation into lipid nanodiscs is an interesting finding in this regard. Obviously, $eNOS_{oxy}$ does not have the reductase domain; therefore the domain-domain opening and closing known in full length NOS that can potentially be affected by the local membrane cannot be in operation here. Also, effects on structural features such as the flexible hinge in the NOS reductase domain that may repress electron transfer to the oxygenase domain may not take part here. Nonetheless, the decreased activity that we observe shows that the nanodisc membrane model represses the basic catalytic function of the dimeric eNOS oxygenase and highlights other effects that modulate eNOS activity beyond the structural elements [40].

In conclusion, we report here for the first time on the successful incorporation and characterization of $eNOS_{oxy}$ on lipid POPC nanodiscs. Our data and analysis show that the activity of eNOS oxygenase on the lipid nanodiscs as a membrane model is ~65% lower compared to free eNOS oxygenase. This nanodisc system provides a model to examine how the local environment and lipid/cholesterol content interact with eNOS oxygenase at the molecular level. Since eNOS is a membrane-associated enzyme, the nanodisc system can be used as a platform where protein-membrane interactions can be studied under controlled conditions. In addition, this system will allow us to address key questions: first, it will allow us to examine how the dynamics of the full-length enzyme are affected by the presence of lipid nanodiscs. Second, with this lipid nanodisc system, we can study if different kinds and levels of phospholipids in membrane compositions have varying effects on eNOS enzyme's molecular function.

Supplementary Material

Refer to Web version on PubMed Central for supplementary material.

Acknowledgments

References

1. Shaul PW, et al. Acylation Targets Endothelial Nitric-oxide Synthase to Plasmalemmal Caveolae. Journal of Biological Chemistry. 1996; 271(11):6518–6522. [PubMed: 8626455]

2. Michel T, Feron O. Nitric oxide synthases: which, where, how, and why? Journal of Clinical Investigation. 1997; 100(9):2146–2152. [PubMed: 9410890]

3. Alderton WK, Cooper CE, Knowles RG. Nitric oxide synthases: structure, function and inhibition. Biochemical Journal. 2001; 357(Pt 3):593–615. [PubMed: 11463332]

4. Govers R, Rabelink TJ. Cellular regulation of endothelial nitric oxide synthase. American Journal of Physiology - Renal Physiology. 2001; 280(2):F193–F206. [PubMed: 11208594]

5. Ohashi Y, et al. Activation of Nitric Oxide Synthase from Cultured Aortic Endothelial Cells by Phospholipids. Biochemical and Biophysical Research Communications. 1993; 195(3):1314–1320. [PubMed: 7692845]

6. Venema RC, et al. Role of the Enzyme Calmodulin-binding Domain in Membrane Association and Phospholipid Inhibition of Endothelial Nitric Oxide Synthase. Journal of Biological Chemistry. 1995; 270(24):14705–14711. [PubMed: 7540177]

7. Davda RK, et al. Oleic Acid Inhibits Endothelial Nitric Oxide Synthase by a Protein Kinase C–Independent Mechanism. Hypertension. 1995; 26(5):764–770. [PubMed: 7591016]

8. Ryan RO. Nanobiotechnology applications of reconstituted high density lipoprotein. Journal of Nanobiotechnology. 2010; 8:28–28. [PubMed: 21122135]

9. Ritchie TK, et al. Reconstitution of Membrane Proteins in Phospholipid Bilayer Nanodiscs. Methods in enzymology. 2009; 464:211–231. [PubMed: 19903557]

10. Bayburt TH, Sligar SG. Single-molecule height measurements on microsomal cytochrome P450 in nanometer-scale phospholipid bilayer disks. Proceedings of the National Academy of Sciences of the United States of America. 2002; 99(10):6725–6730. [PubMed: 11997441]

11. Nath A, Atkins WM, Sligar SG. Applications of Phospholipid Bilayer Nanodiscs in the Study of Membranes and Membrane Proteins. Biochemistry. 2007; 46(8):2059–2069. [PubMed: 17263563]

12. Das A, Sligar SG. Modulation of the Cytochrome P450 Reductase Redox Potential by the Phospholipid Bilayer. Biochemistry. 2009; 48(51):12104–12112. [PubMed: 19908820]

13. Baker SE, et al. Hydrogen Production by a Hyperthermophilic Membrane-Bound Hydrogenase in Water-Soluble Nanolipoprotein Particles. Journal of the American Chemical Society. 2009; 131(22):7508–7509. [PubMed: 19449869]

14. Driessen AJM, Nouwen N. Protein Translocation Across the Bacterial Cytoplasmic Membrane. Annual Review of Biochemistry. 2008; 77(1):643–667.

15. Raschle T, et al. Structural and functional characterization of the integral membrane protein VDAC-1 in lipid bilayer nanodiscs. Journal of the American Chemical Society. 2009; 131(49): 17777–17779. [PubMed: 19916553]

16. Cruz F, Edmondson ED. Kinetic properties of recombinant MAO-A on incorporation into phospholipid nanodisks. Journal of Neural Transmission. 2007; 114(6):699–702. [PubMed: 17393065]

17. Gachhui R, et al. Mutagenesis of Acidic Residues in the Oxygenase Domain of Inducible Nitric-Oxide Synthase Identifies a Glutamate Involved in Arginine Binding. Biochemistry. 1997; 36(17): 5097–5103. [PubMed: 9136868]

18. Stuehr DJ, et al. N omega-hydroxy-L-arginine is an intermediate in the biosynthesis of nitric oxide from L-arginine. J Biol Chem. 1991; 266(10):6259–63. [PubMed: 1706713]

19. Denisov IG, et al. Cooperativity in Cytochrome P450 3A4: Linkages in substrate binding, spin state, uncoupling, and product formation. Journal of Biological Chemistry. 2007; 282(10):7066–7076. [PubMed: 17213193]

20. Raman CS, et al. Crystal Structure of Constitutive Endothelial Nitric Oxide Synthase. Cell. 95(7): 939–950. [PubMed: 9875848]

21. Mazhab-Jafari MT, et al. Oncogenic and RASopathy-associated K-RAS mutations relieve membrane-dependent occlusion of the effector-binding site. Proceedings of the National Academy of Sciences of the United States of America. 2015; 112(21):6625–6630. [PubMed: 25941399]

22. Streletzky KA, McKenna JT, Mohieddine R. Spectral time moment analysis of microgel structure and dynamics. Journal of Polymer Science Part B: Polymer Physics. 2008; 46(8):771–781.

23. Phillies, GDJ., K, AS. Dynamics of Semirigid Polymers from Experimental Studies. In: Dillon, K., editor. Soft Condensed Matter: New Research. Nova Science; New York: 2007.

24. Denisov IG, et al. Directed Self-Assembly of Monodisperse Phospholipid Bilayer Nanodiscs with Controlled Size. Journal of the American Chemical Society. 2004; 126(11):3477–3487. [PubMed: 15025475]

25. Philo JS. Is any measurement method optimal for all aggregate sizes and types? The AAPS Journal. 2006; 8(3):E564–E571. [PubMed: 17025274]

26. Demeule B, et al. New methods allowing the detection of protein aggregates: A case study on trastuzumab. mAbs. 2009; 1(2):142–150. [PubMed: 20061815]

27. Nobbmann U, et al. Dynamic light scattering as a relative tool for assessing the molecular integrity and stability of monoclonal antibodies. Biotechnology and Genetic Engineering Reviews. 2007; 24(1):117–128. [PubMed: 18059629]

28. Bayburt TH, et al. Monomeric Rhodopsin Is Sufficient for Normal Rhodopsin Kinase (GRK1) Phosphorylation and Arrestin-1 Binding. The Journal of Biological Chemistry. 2011; 286(2):1420–1428. [PubMed: 20966068]

29. Bayburt TH, et al. Transducin Activation by Nanoscale Lipid Bilayers Containing One and Two Rhodopsins. Journal of Biological Chemistry. 2007; 282(20):14875–14881. [PubMed: 17395586]

30. Wei C-C, et al. The Three Nitric-oxide Synthases Differ in Their Kinetics of Tetrahydrobiopterin Radical Formation, Heme-Dioxy Reduction, and Arginine Hydroxylation. Journal of Biological Chemistry. 2005; 280(10):8929–8935. [PubMed: 15632185]

31. Adak S, Wang Q, Stuehr DJ. Arginine Conversion to Nitroxide by Tetrahydrobiopterin-free Neuronal Nitric-oxide Synthase: IMPLICATIONS FOR MECHANISM. Journal of Biological Chemistry. 2000; 275(43):33554–33561. [PubMed: 10945985]

32. Robinson LJ, Busconi L, Michel T. Agonist-modulated palmitoylation of endothelial nitric oxide synthase. J Biol Chem. 1995; 270(3):995–8. [PubMed: 7530714]

33. Schilling K, et al. Translocation of endothelial nitric-oxide synthase involves a ternary complex with caveolin-1 and NOSTRIN. Mol Biol Cell. 2006; 17(9):3870–80. [PubMed: 16807357]

34. Garcia-Cardena G, et al. Targeting of nitric oxide synthase to endothelial cell caveolae via palmitoylation: implications for nitric oxide signaling. Proc Natl Acad Sci U S A. 1996; 93(13):6448–53. [PubMed: 8692835]

35. Venema RC, et al. Role of the enzyme calmodulin-binding domain in membrane association and phospholipid inhibition of endothelial nitric oxide synthase. J Biol Chem. 1995; 270(24):14705–11. [PubMed: 7540177]

36. Jin Z-G. Where Is Endothelial Nitric Oxide Synthase More Critical: Plasma Membrane or Golgi? Arteriosclerosis, Thrombosis, and Vascular Biology. 2006; 26(5):959–961.

37. Murphy EJ, et al. Phospholipid composition of cultured human endothelial cells. Lipids. 1992; 27(2):150–153. [PubMed: 1315902]

38. Govers R, Rabelink TJ. Cellular regulation of endothelial nitric oxide synthase. Am J Physiol Renal Physiol. 2001; 280(2):F193–206. [PubMed: 11208594]

39. Zhang Q, et al. Functional Relevance of Golgi- and Plasma Membrane-Localized Endothelial NO Synthase in Reconstituted Endothelial Cells. Arteriosclerosis, Thrombosis, and Vascular Biology. 2006; 26(5):1015–1021.

40. Haque MM, et al. A connecting hinge represses the activity of endothelial nitric oxide synthase. Proc Natl Acad Sci U S A. 2007; 104(22):9254–9. [PubMed: 17517617]

Abbreviations

eNOS$_{oxy}$	endothelial nitric oxide synthase oxygenase domain
MSP	membrane scaffold protein
DLS	dynamic light scattering
POPC	palmitoyl-2-oleoyl-sn-glycero-3-phosphocholine

Highlights

- Endothelial nitric oxide synthase (eNOS) is a membrane-anchored enzyme with a distinctly low nitric oxide synthesis activity involved, in vasodilation and maintaining vascular tone.

- All work published so far on eNOS about the molecular function and activity of eNOS is on a recombinant version that is soluble and not attached to a membrane.

- We have successfully incorporated and characterized the recombinant oxygenase subunit of the enzyme into lipid nanodiscs as a membrane model.

- This is the first study that highlights the modulation of eNOS activity by the nano-sized membrane as modeled by lipid nanodiscs.
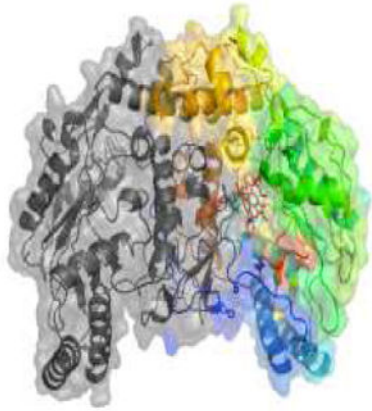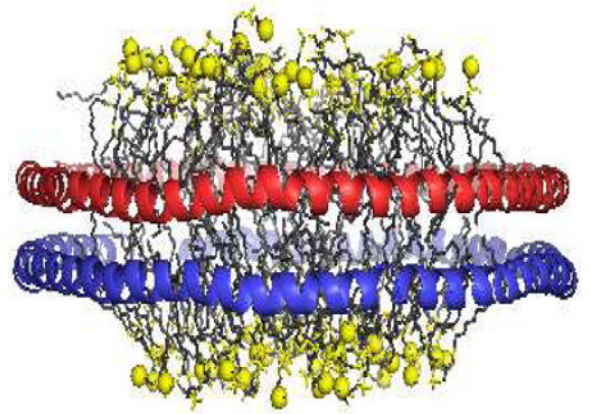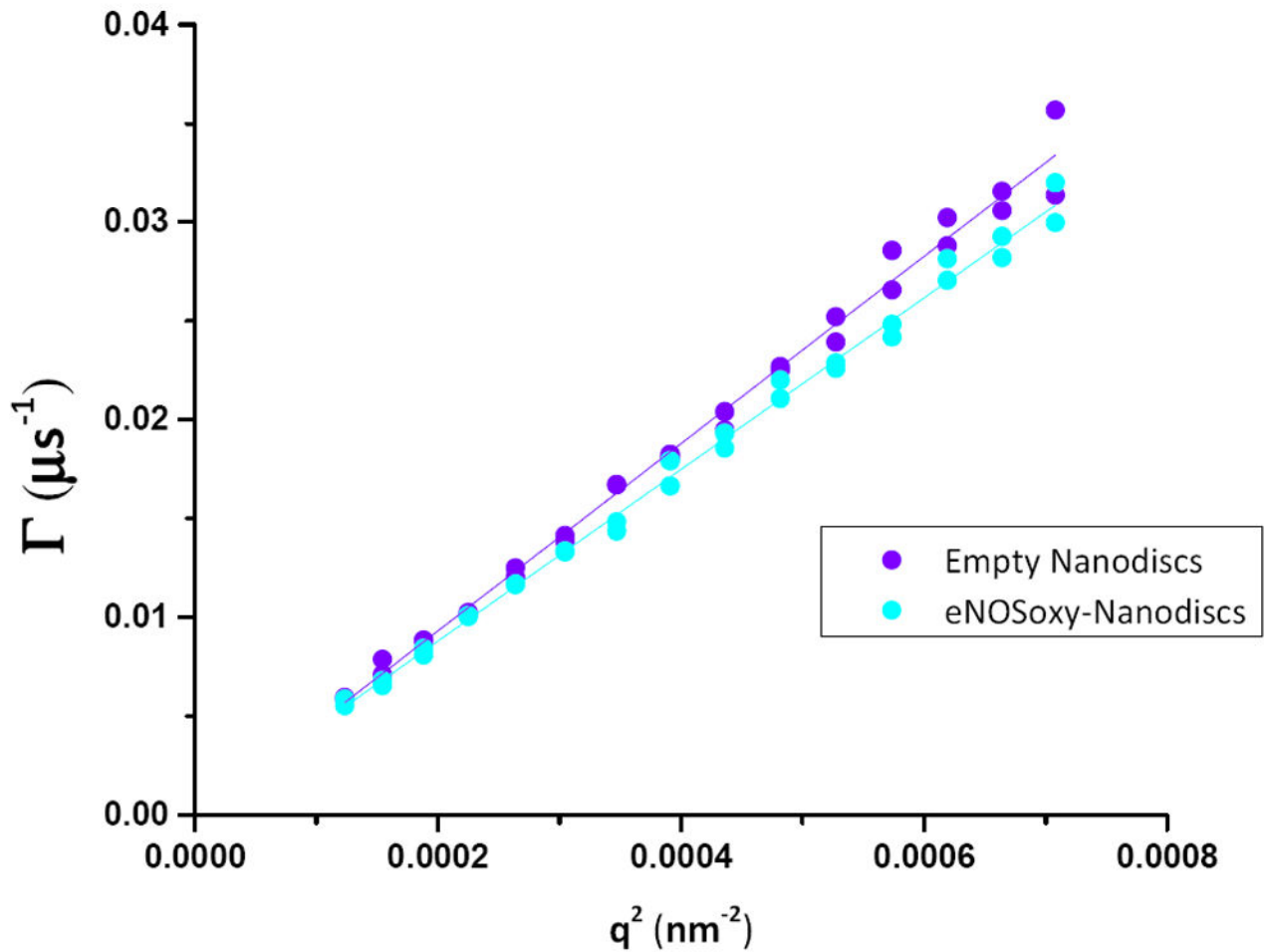
Figure 1.
A: Schematic representation of eNOS oxygenase domain dimer (PDB ID 1NSE) using PyMOL adapted from Protein Data Bank [20]. The oxygenase domain carries a prosthetic heme group and binds the cofactor (6R-)5,6,7,8-tetrahydrobiopterin (BH$_4$) as well as molecular oxygen (O$_2$) and L-arginine. B: Representation of assembled nanodisc (PDB ID 2MSC) using PyMOL adapted from Protein Data Bank [21]. The nanodisc discoidal structure consists of two membrane scaffold proteins (red and blue) that cover the hydrophobic alkyl chains of each phospholipid leaflet in the bilayer domain.
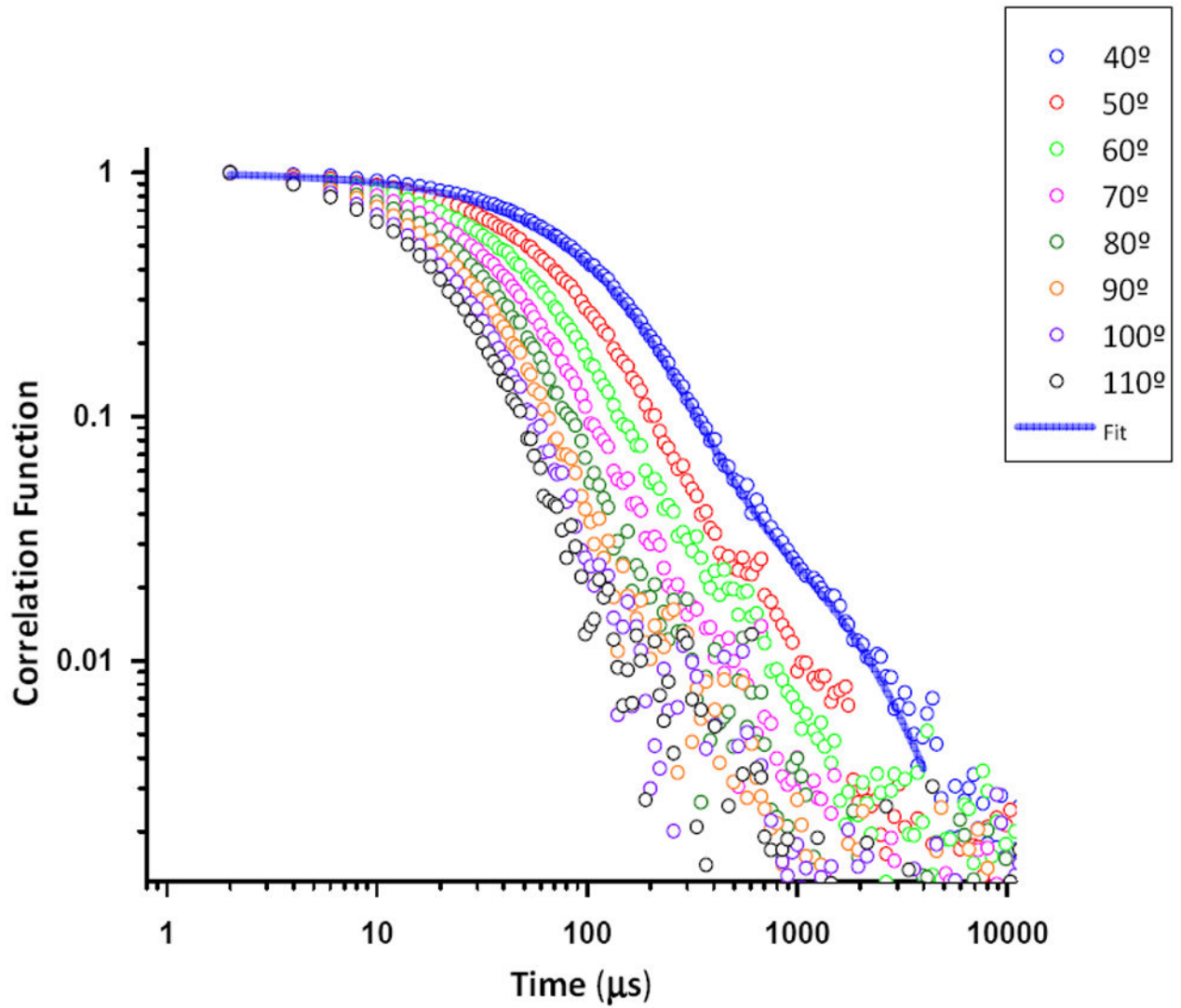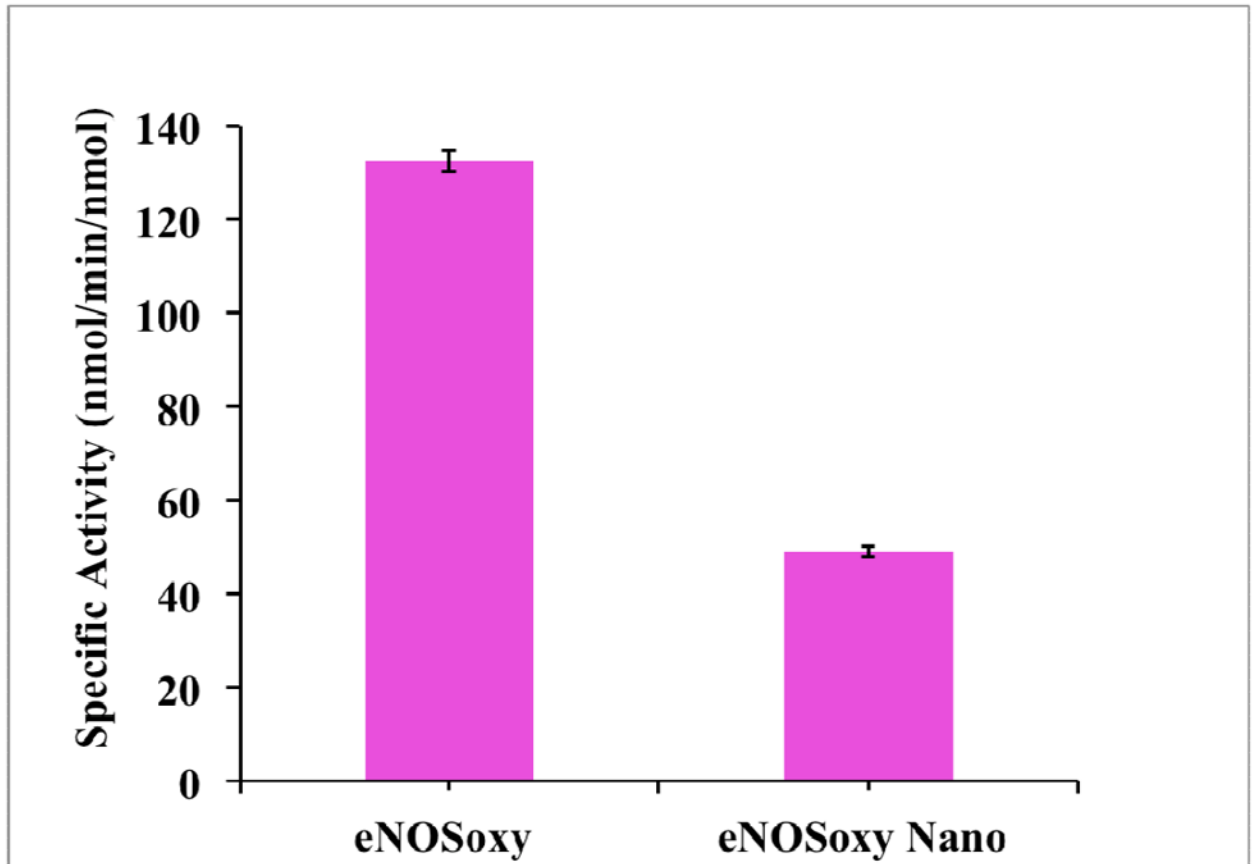
Figure 2.
Measured normalized correlation functions of empty nanodisc sample plotted for angle range θ =40–110°. The correlation functions of both nanodiscs and $eNOS_{oxy}$/nanodiscs samples were reproducible and covered almost three decades of a decay indicating strong scattering and found to demonstrate strong angular dependence, consistent with translational motion of diffusive species.

Figure 3.
DLS measured decay rate (Γ) as a function of (q^2) for eNOS$_{oxy}$/nanodiscs and empty nanodiscs. Both samples yielded two modes, the faster mode shown on Figure 3 had diffusive behavior of particles with 70-80% contribution to the correlation function and small intercepts < 0.5 %, almost pure exponential decays. The slower mode had non-diffusive behavior indicating aggregates.

Figure 4.
Comparison of Specific activity values of eNOS$_{oxy}$/nanodisc and free eNOS$_{oxy}$. The specific activity of eNOS$_{oxy}$/nanodisc or free eNOSoxy is calculated in nmol NO released in the form of nitrite per min per nmol of enzyme at 37°C. Values represent the mean and standard deviations of three independent measurements.